Visualization of Molecular Fluctuations near the Critical Point of the Coil–Stretch Transition in Polymer Elongation

Hazen P. Babcock,[†] Rodrigo E. Teixeira,[†,‡] Joe S. Hur,[‡] Eric S. G. Shaqfeh,[§] and Steven Chu*,[†]

Departments of Physics and Applied Physics, Varian Building, Stanford University; Department of Chemical Engineering, Stauffer III, Stanford University; and Departments of Chemical and Mechanical Engineering, Stauffer III, Stanford University, Stanford, California 94305

ABSTRACT: The coil–stretch transition in the extension of polymers in two-dimensional flows was investigated near a critical boundary defined by simple shear flow. Visualization of individual molecules revealed a sharp coil–stretch transition in the steady-state length of the polymer with increasing Weissenberg number (Wi) in flows where the magnitude of the elongational component ($||E||$) slightly exceeded the rotational component ($||\Omega||$). However, unlike in pure elongational flow, large fluctuations in the length of the polymer were observed near the critical point of the transition. These fluctuations result in a "softening" of the phase transition between coiled and extended states of the polymer. In flows where $||\Omega||$ is slightly greater than $||E||$, significant transient polymer deformation was observed. However, the average length of the polymer as a function of Wi increased much more slowly than in simple shear flow.

Introduction

In a seminal paper in 1974, de Gennes proposed a phase diagram for arbitrary two-dimensional flows.[1] These flows can always be factored into an elongational component E, where neighboring fluid elements separate exponentially with time, and a rotational component, Ω, where fluid elements rotate with time. Polymers in flows where $||E|| > ||\Omega||$ would exhibit a sharp coil-to-stretched transition if Wi exceeds a critical value. In the limit of long polymers the transition would be discontinuous (first order). As $||E||$ approached $||\Omega||$ from above, de Gennes asserted that this coil–stretch transition would "soften". In the special case of simple shear flow ($||E|| = ||\Omega||$), the sharp transition would vanish. In flows where $||E|| < ||\Omega||$, polymers would remain coiled regardless of Wi. De Gennes' predictions triggered extensive investigations into the conformational changes of polymers induced by these types of flow. In particular, the limiting cases of purely elongation flow ($||\Omega|| = 0$) and shear flow were heavily studied.

Experiments in purely elongational flow based on optical birefringence (reviewed in refs 2 and 3) suggested that the polymers reached equilibrium in a highly extended state. Measurements of extensional viscosities in filament stretching experiments[4,5] also showed that these flows were stretching the polymers. However, the measured stress due to filament extension[6] indicated that the polymers were not reaching full extension. Light scattering[7] (and references contained therein) experiments showed that polymers were barely deformed in flow strengths high enough to saturate the birefringence signal. These conflicts were finally resolved in favor of De Gennes' prediction by imaging single polymers of DNA in extensional flows.[8–10] The ability to observe the real-time extension of each molecule showed that previous ensemble measurements blurred the inherently sharp phase transition by averaging over many molecules where a significant fraction of them had not yet reached their equilibrium extension.

Light scattering and neutron experiments on polymers in simple shear flows suggested that these flows were not deforming the polymer significantly.[11–14] In agreement with de Gennes' predictions, however, the direct measurement of individual polymer extension in simple shear flow by single molecule techniques revealed that the average extension of the polymers was increasing with Wi. Furthermore, it was found that the molecular extension did not show a sharp transition with increasing velocity gradient, continued to fluctuate in time, and *never* reached an equilibrium state.[15] These fluctuations, difficult to detect with observations of an ensemble of molecules, were easily observed with single molecule imaging methods.

The existence of a coil–stretch transition in general two-dimensional flows where $||E|| > ||\Omega||$ has been treated theoretically[16–20] and probed experimentally with optical birefringence by Leal and collaborators.[21–24] The birefringence signal was observed to approach saturation with increasing Wi, indicating the polymers were nearing the fully stretched state. They found that the birefringence signal could be collapsed by rescaling the flow strength with the flow type parameter λ. However, when the birefringence was plotted in terms of this rescaled, dimensionless velocity gradient, the transition from the coiled to stretched state for all flows was fairly gradual, starting at ~2 and still increasing at ~38 (see for example Figure 15 of ref 22).

One question that was not addressed by the earlier birefringence studies of mixed flows was how the transition from coiled to stretched state might "soften" as $||E||$ approached $||\Omega||$, since those studies did not observe a sharp transition in either pure extensional or mixed flows. In this paper we report the first single molecule visualization of the polymer dynamics involved in the coil–stretch transition in the region of the phase diagram where $||E||$ is either slightly greater or less than

---

[†] Departments of Physics and Applied Physics.
[‡] Department of Chemical Engineering.
[§] Departments of Chemical and Mechanical Engineering.
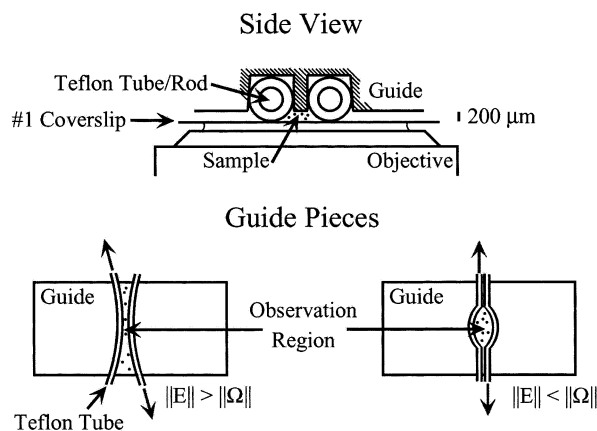* Corresponding author.

Side View

Guide Pieces

Figure 1. The top panel is a side view, showing the relative position of the guide piece, tubes/rods, sample, coverslip (#1), and objective (1.2 NA 60× Water Immersion, Nikon). The bottom panel shows guide pieces with different groove patterns for $\lambda > 0$ or $\lambda < 0$.

$||\Omega||$. These studies are the first to give us a detailed microscopic understanding of how the coil−stretch phase transition "softens" for arbitrary two-dimensional flows that approach simple shear flow.

Experimental Section

Apparatus. We constructed a novel apparatus that produced flows close to simple shear and that allowed fluorescence imaging of single polymers (see Figure 1). Moving tubes (0.034 in. diameter Teflon) or rods (0.032 in. diameter Teflon) were used to create flows with the desired properties. The tubes/rods were held under tension and translated in opposite directions by an external apparatus (not shown). The tubes/rods ran in grooves machined into an acrylic plastic guide that defined the flow type. The gap between the guide and coverslip was 200 μm (see the upper panel of Figure 1). Guides with different groove patterns were made to create flows where $||E|| > ||\Omega||$ or $||E|| < ||\Omega||$, illustrated in the lower panels of Figure 1.

For each guide the flow type created was determined 3−6 times by tracking 1um fluorescent beads. Each time, a data set of bead position (bx_n, by_n) and velocity $(bv_{n,x}, bv_{n,y})$ was measured. This data set consisted of >1000 data points spread out over a large area so that flow type could be determined with high precision even when the flow was very close to simple shear. Parts of some of the data sets are shown in Figure 2A−D. This data set was used to calculate a flow matrix $[\nabla V]$ by least-squares minimization of

$$\begin{bmatrix} bv_{n,x} \\ bv_{n,y} \end{bmatrix} = [\nabla V] \begin{bmatrix} bx_n - x_0 \\ by_n - y_0 \end{bmatrix}$$

where x_0 and y_0 are free parameters. Then from $[\nabla V]$,

$$E = \frac{1}{2}(\nabla V + \nabla V^T), \quad \Omega = \frac{1}{2}(\nabla V - \nabla V^T),$$

$$||E|| \equiv \sqrt{\frac{1}{2}\sum_i\sum_j E_{i,j}^2}, \quad ||\Omega|| \equiv \sqrt{\frac{1}{2}\sum_i\sum_j \Omega_{i,j}^2}$$

were calculated. λ was calculated using

$$\lambda = \frac{||E|| - ||\Omega||}{||E|| + ||\Omega||}$$

Three different guide pieces were used with flow type parameter (λ) of $\lambda = (15.9 \pm 1.1) \times 10^{-3}$ (tubes, guide 1), $\lambda = (4.8 \pm 0.5) \times 10^{-3}$ (tubes, guide 2), and $\lambda = (-6.2 \pm 0.7) \times 10^{-3}$ (tubes, guide 3) or $\lambda = (-9.2 \pm 0.5) \times 10^{-3}$ (rods, guide 3).

Bead tracking also showed that the apparatus was capable of producing a stable and linear two-dimensional flow. Linear-
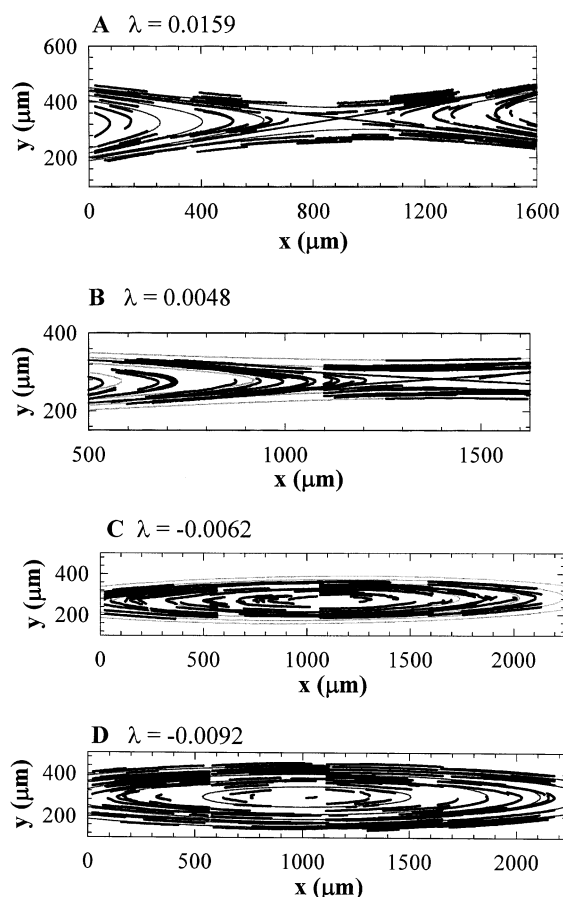

Figure 2. Beads were tracked in several fields of view at 30 Hz video rate with a 20× air objective (Nikon). The points are beads that were followed for >100 frames. The solid lines are the streamlines (dark gray) and eigenvectors (black) of $[\nabla V]$. The location of the origin is arbitrary. (A) A flow with $\lambda = 15.9 \times 10^{-3}$, (B) a flow with $\lambda = 4.8 \times 10^{-3}$, (C) a flow with $\lambda = -6.2 \times 10^{-3}$, and (D) a flow with $\lambda = -9.2 \times 10^{-3}$.

ity is illustrated by Figure 3A where average bead velocities vs distance from the stagnation point are shown. Linearity was further studied by comparing the measured bead velocities to the bead velocities calculated from the best fit flow matrix. In this way it was found that the flow was linear to better than 10% over a region that is 9 times larger than that in which polymers were studied. The stability of the apparatus was measured, and representative data are shown in Figure 3B. The strain rate $\Gamma \equiv ||E|| + ||\Omega||$ was found to vary by less than 5% rms over the time course of an experiment.

To verify that the fluctuations observed in Figure 3A,B are real, the bead tracking algorithm was tested with simulated data. Flow matrices were used to generate bead position and velocity data for a total number of tracked beads per image comparable to that seen in the real data. In this way it was found that the tracking algorithm could determine the linearity and the strain rate to 1%. The observed fluctuations are almost entirely due to defects in the Teflon tubes as the motion of the external apparatus responsible for their translation was observed directly and found to be stable to better than 1%.

Materials. The polymers studied were fluorescently labeled lambda bacteriophage DNA (λ-DNA) containing ~440 persistence lengths. The dye YOYO-1 (Molecular Probes) was used at 1:4 dye to base-pair ratio to stain the λ-DNA (Gibco). When stained, the λ-DNA has a contour length of 22 μm.[25] The persistence length of native DNA is ~53 nM, and its hydrodynamic radius is ~2 nM.[26,27] λ-DNA was suspended in one of two different viscous sugar solutions that were similar to those used previously:[8,15] 10 mM Tris buffer pH 8.0, 10 mM NaCl, 1 mM EDTA, and sucrose (40−50% w/v) to increase viscosity. An oxygen scavenging system consisting of glucose (10% w/v),
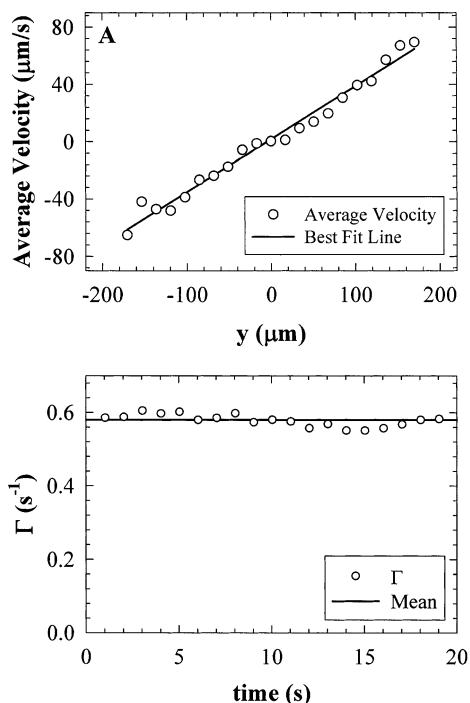
Figure 3. Data were taken using guide 1 and Teflon tubes. (A) The average bead velocity in 17 μm bins (circles) is plotted for beads whose x position was within 100 μm of the stagnation point (x and y are as defined in Figure 2A−D). The line is the best fit line. (B) Beads were tracked continuously for 20 s in a single field of view centered on the stagnation point. 1 s snapshots of bead tracking data were then used to determine Γ. The line is the average Γ.

glucose oxidase (0.05 mg/mL), catalase (0.01 mg/mL), and β-mercaptoethanol (1% v/v) was used to reduce photobleaching.

The viscosity of the buffers was measured using a cone−plate viscometer and was found to be 25 and 100 cP, respectively, at 23 °C. We believe, however, that the actual viscosity of the solutions when loaded into the apparatus is approximately 50 and 200 cP, respectively. This belief is based on a comparison of the measured polymer relaxation time, τ, with previous values of τ obtained in earlier experiments at different viscosities done in this lab. We think the difference in viscosity seen in this experiment can be attributed in part to a 3−5 °C temperature difference between the lab where the viscosity was measured and the lab where the data were taken and in part to solvent evaporation during the 5 min that it took to load the sugar solution into the apparatus. After the solution had been loaded the apparatus was sealed, and no significant difference was detected in τ measured before and after an experimental run (typically of 2 h in length). The average τ was also consistent from run to run.

General. The Wi of a flow was determined using the formula $Wi = \Gamma\tau$ (τ is the longest polymer relaxation time). The strain rate Γ was determined by the speed of an external dc encoded motor (Maxon Motors) which translated the tubes/rods. The relaxation time τ was determined by fitting the relaxation of >50 molecules to the function $x(t)^2 = c\exp(-t/\tau) + 4R_g^2$, where $x(t)$ is the extension and τ, C, and R_g^2 are free parameters in the fit: τ was measured to be 4.7 s in the 50 cP buffer and 20 s in the 200 cP buffer used for these experiments.

The polymers were imaged using a home-built inverted microscope setup for epi-fluorescence. This microscope used a 100 W mercury arc lamp (Zeiss), a 470 ± 32 nm band-pass excitation filter (Chroma), and a 500 nm long-pass dichroic (Chroma) to excite the fluorescent dye. A 60×, 1.2 numerical aperture water immersion microscope objective (Nikon) was used both to couple in the excitation light and to image the resulting fluorescence. Additionally, the imaging pathway contained a 160 mm-to-infinity-corrected conversion lens (Zeiss), a 40 cm tube lens (Newport), a 515 nm long pass
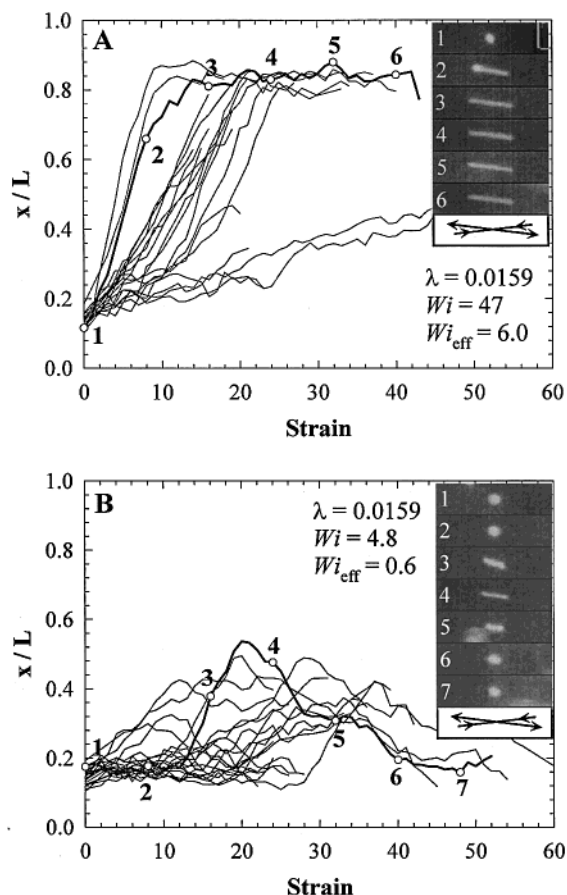

Figure 4. Plots of fractional extension (x/L) vs strain (Γt) for different polymer molecules exposed to a sudden flow. 4−8 measurements of x/L were made per unit of strain and averaged. The upper insets each show an image of the polymer whose fractional extension is given by the heavy black line. The numbers on the x/L trace correspond to the numbers in the images. Each image is a 1 strain unit average of the movie. The lower inset shows the orientation of the eigenvectors of $[\nabla V]$. (A) $\lambda = 15.9 \times 10^{-3}$ and $Wi = 47$. (B) $\lambda = 15.9 \times 10^{-3}$ and $Wi = 4.8$.

emission filter (Chroma), and a video camera (Phillips 600TN CCD) fiber coupled to a microchannel plate intensifier (Hamamatsu).

The polymers were imaged at a depth of 120 ± 20 μm in the apparatus, where velocity gradients in the z-direction were found to be minimal. Movies of polymer behavior were captured directly to a computer from the video camera using a National Instruments frame grabber card (PCI-1407). The polymer extension in each frame of a movie was determined using a threshold-based algorithm. The results of the algorithm were checked and corrected manually.

Results and Discussion

The behavior of 20−26 polymers was recorded at each value of Wi and λ. Starting from equilibrium in the absence of flow, a movie of a polymer was recorded until it was carried out of the observation area. Data taken at $Wi = 47$ and $\lambda = 15.9 \times 10^{-3}$ are shown in Figure 4A. The extension (x) starts at that of a coil and approaches the contour length (L) as the flow stretches the polymer. The amount of strain necessary to reach an equilibrium extension was different for physically identical polymers. The heterogeneous extension is due to the initial polymer conformation, similar to the behavior previously observed in purely elongational flow ($\lambda = 1.0$).[8,9]

The inset in Figure 4A shows successive images of the polymer at different points in the black line time trajectory. The observation that all the polymers align with maximal extension along a well-defined direction has an immediate geometric interpretation. Instead of considering the flow as a sum of pure elongational and rotational flows, these observations instruct us to analyze the polymer behavior in terms of the eigenvectors of the flow matrix $[\nabla V]$. One of the eigenvectors corresponds to the extensional axis in which the fluid elements stretch and makes an angle $\tan \theta/2 = +\sqrt{\lambda}$ with respect to the horizontal. The polymers achieve their maximum extension along this axis. The other eigenvector oriented with $\tan \theta/2 = -\sqrt{\lambda}$ corresponds to the compression axis. In a purely extensional flow ($\lambda = 1$), the two eigenvectors are at $\theta = \pm 45°$.

The eigenvalue of $[\nabla V]$ sets the scale of the velocity gradient along the extensional axis. On the basis of this observation and following previous work,[21,22] we rescale $||E|| > ||\Omega||$ data for different λ by defining a $Wi^{\text{eff}} = \sqrt{\lambda} Wi$, so that the flow along the extensional eigenvector is rescaled by the magnitude of $||E||$.

Large fluctuations were seen in polymer extension at lower Wi in flows where the angle θ is small, indicative of a softening of the coil−stretch transition as $||E||$ approaches $||\Omega||$ (see Figure 4B). As shown by the polymer depicted in the insets, the extension increased when the polymer was aligned with the outgoing eigenvector (inset 3). Eventually, Brownian motion "kicks" the polymer out of this orientation, typically aligning roughly horizontally between the eigenvectors of ∇V (inset 5). Here the flow exerts little stretching force, and the polymer can collapse to a coiled state (inset 6). These fluctuations were not seen in pure elongational flow where, instead, at the same Wi^{eff} (=0.6), x/L fluctuated only slightly around 0.5.[8]

Note that simple shear flow ($\lambda = 0$, $\theta = 0$) guarantees that the configuration of the polymer will never reach a stable equilibrium. In this flow the extension and compression eigenvectors are parallel to each other. An extended polymer will align with these eigenvectors; then an infinitesimal thermal fluctuation can rotate the polymer into a orientation which will cause the polymer to coil.

Figure 5A shows that a small change in λ has a large effect on the polymer's dynamics. The polymer was aligned and stretched by flows with $\lambda > 0$. The mean extension rapidly approaches the contour length with Wi (upper three traces). If the maximum elongation along the extension eigenvector is taken as the effective "steady-state extension" of the polymer, the only relevant quantity that determines the coil−stretch transition should be the normalized flow strength Wi^{eff}. A plot of the polymer extension vs Wi^{eff} for flows where $\lambda = 1.0$, 0.0159, and 0.0048 follows a universal extension curve, as shown in Figure 5B. Thus, the coil−stretch transition persists even in flows very near simple shear. Our result amplifies earlier experimental and theoretical work that showed that polymer birefringence data could be collapsed in a similar manner.[16−18,21,22] In the current work, however, the transition is found to be over an order of magnitude sharper than previously observed, even for values of λ much closer to $\lambda = 0$.

We have also studied polymer behavior in the previously unexplored region of phase space where $\lambda < 0$ ($||E|| < ||\Omega||$). For $\lambda = -0.0062$, modest but significant polymer extension is seen (Figure 5A). These deforma-
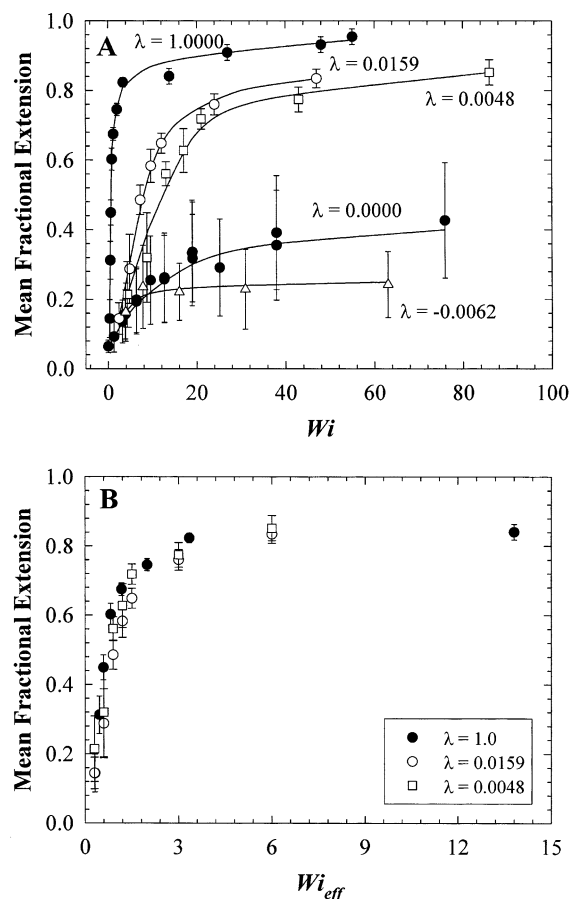

Figure 5. Mean fractional maximum extension along the extensional eigenvector vs Wi for $\lambda > 0$ and $Wi^{\text{eff}} > 0.6$. For $Wi^{\text{eff}} \leq 0.6$, the average extension after 20 strain units is plotted. $\lambda = 1.0$ and $\lambda = 0.0$ data are from refs 7, 8, and 14. Error bars are standard deviations in the mean, to show the size of fluctuations in extension, except for $\lambda = 1.0$ where they are errors in the mean. (A) Polymer mean fractional extension vs Wi for five different flow types. The lines are guides for the eye. (B) Polymer mean fractional extension plotted as a function of the Wi^{eff} for flows with $\lambda > 0$.

tions are due to the elliptical nature of $\lambda < 0$ flow. Even though neighboring fluid elements never separate by more than a finite amount, they separate sufficiently far to deform a polymer.

These deformations are periodic, reflecting the underlying periodicity of $\lambda < 0$ flows. Figure 6 shows a peak in the power spectra of polymer extension data taken in such flows. Such a peak was clearly visible for $\lambda = -9.2 \times 10^{-3}$ but was less apparent for $\lambda = -6.2 \times 10^{-3}$. In agreement with our experiment, Brownian dynamics simulations predict that the power at twice the rotation frequency should be $\sim$10 times that in neighboring frequencies for $\lambda = -9.2 \times 10^{-3}$, but only $\sim$2 times for $\lambda = -6.2 \times 10^{-3}$.[28]

Conclusion

The observation of individual molecules has allowed us to follow the coil−stretch transition as the flow parameter $\lambda \rightarrow 0$ from either positive or negative values of λ. For $\lambda > 0$ flows, a sharp, universal extension curve was found down to $\lambda = 0.0048$ and $Wi^{\text{eff}} \geq \sim$0.6. The observation that the molecules align along an eigenvector of the flow matrix reveals how the coil−stretch phase transition softens due to Brownian dynamics: fluctuations are required to "kick" the polymer out of alignment
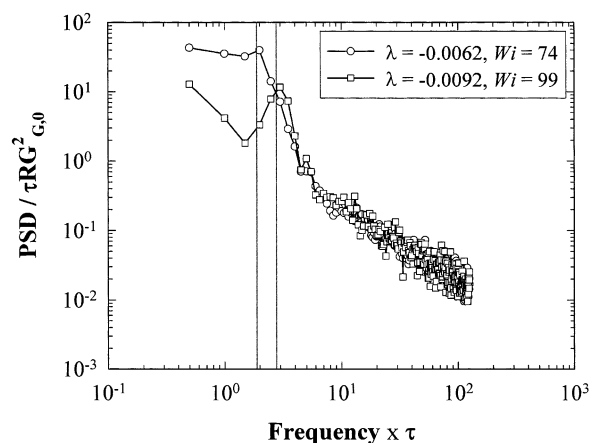
Figure 6. Dimensionless power spectral densities (PSDs) of polymer extension in $\lambda < 0$ flow. R_G is the polymer radius of gyration. PSDs were calculated as in ref 14. To minimize start-up transients, the first 40 strain units of data were not included in the calculation. The gray lines indicate the frequency of the flow (left, $\lambda = -6.2 \times 10^{-3}$; right, $\lambda = -9.2 \times 10^{-3}$).

with the extensional eigenvector. We anticipate that longer polymers would exhibit a sharp transition for much smaller angles between the extension and compression eigenvectors, and the phase transition as λ approaches 0 may be described in terms of a critical exponent.[29] When $\lambda < 0$, significant transient deformation of the polymer occurs due to the elliptical nature of the flow.

References and Notes

(1) De Gennes, P. G. *J. Chem. Phys.* **1974**, *60*, 5030.
(2) Carrington, S. P.; Odell, J. A. *J. Non-Newtonian Fluid Mech.* **1996**, *67*, 269.
(3) Odell, J. A.; Carrington, S. P. *Flexible Polymer Chains in Elongational Flow*; Nguyen, T. Q., Kausch, H. H., Eds.; Springer: Berlin, 1999; pp 137−182.
(4) Tirtaatmadja, V.; Sridhar, T. *J. Rheol.* **1993**, *37*, 1081.
(5) Spiegelberg, S. H.; McKinley, G. H. *J. Non-Newtonian Fluid Mech.* **1996**, *67*, 49.
(6) James, D. F.; Sridhar, T. *J. Rheol.* **1995**, *39*, 713.
(7) Menasveta, M. J.; Hoagland, D. *Macromolecules* **1991**, *24*, 3427.
(8) Perkins, T. T.; Smith, D. E.; Chu, S. *Science* **1997**, *276*, 2016.
(9) Smith, D. E.; Chu, S. *Science* **1998**, *281*, 1335.
(10) Perkins, T. T.; Smith, D. E.; Chu, S. *Flexible Polymer Chains in Elongational Flow*; Nguyen, T. Q., Kausch, H. H., Eds.; Springer: Berlin, 1999; pp 283−332.
(11) Cottrell, F.; Merrill, E.; Smith, K. *J. Polym. Sci., Polym. Phys. Ed.* **1969**, *7*, 1415.
(12) Link, A.; Springer, J. *Macromolecules* **1993**, *26*, 464.
(13) Lee, E. C.; Solomon, M. J.; Muller, S. J. *Macromolecules* **1997**, *30*, 7313.
(14) Lindner, P.; Oberthur, R. *Colloid Polym. Sci.* **1988**, *266*, 886.
(15) Smith, D. E.; Babcock, H. P.; Chu, S. *Science* **1999**, *283*, 1724.
(16) Fuller, G. G.; Leal, L. G. *J. Non-Newtonian Fluid Mech.* **1981**, *8*, 271.
(17) Phan-Thien, N.; Manero, O.; Leal, L. G. *Rheol. Acta* **1984**, *23*, 151.
(18) Larson, R. G.; Magda, J. J. *Macromolecules* **1989**, *22*, 3004.
(19) Ng, R. C.-Y.; Leal, L. G. *Rheol. Acta* **1993**, *32*, 25.
(20) Remmelgas, J.; Leal, L. G. *J. Non-Newtonian Fluid Mech.* **2000**, *89*, 231.
(21) Fuller, G. G.; Leal, L. G. *Rheol. Acta* **1980**, *19*, 580.
(22) Dunlap, P. N.; Leal, L. G. *J. Non-Newtonian Fluid Mech.* **1987**, *23*, 5.
(23) Ng, R. C.-Y.; Leal, L. G. *J. Rheol.* **1993**, *37*, 443.
(24) Harrison, G. M.; Remmelgas, J.; Leal, L. G. *J. Rheol.* **1998**, *42*, 1039.
(25) Perkins, T. T.; Smith, D. E.; Larson, R. G.; Chu, S. *Science* **1995**, *268*, 83.
(26) Bustamante, C.; Marko, J.; Siggia, E.; Smith, S. *Science* **1994**, *265*, 1599.
(27) Pecora, R. *Science* **1991**, *251*, 893.
(28) Hur, J. S.; Shaqfeh, E. S. G.; Babcock, H. P.; Chu, S. *Phys. Rev. E* **2002**, *66*, #011915 1-4.
(29) De Gennes, P. G. *Scaling Concepts in Polymer Physics*; Cornell University Press: Ithaca, NY, 1979.

MA034073P